Hindawi
Scientific Programming
Volume 2022, Article ID 4639555, 9 pages
https://doi.org/10.1155/2022/4639555

Research Article

Simulation Analysis of Combined Mechanics of the Thrust Rotary Guide Drill

Bo Zeng,[1] Youcheng Zheng,[2] Pengcheng Wu,[1] Feng Zhou,[3] Mei Huang,[2] Yuxin Bai,[4] Yangyang Gao,[4] and Chengyu Xia[5]

[1]*Shale Gas Research Institute of Petro China Southwest Oil and Gas Field, Chengdu, Sichuan 610051, China*
[2]*PetroChina Southwest Oil & Gas Field Company, Chengdu, Sichuan 610051, China*
[3]*Sichuan Shale Gas Exploration and Development Company Limited, Chengdu, Sichuan 610051, China*
[4]*Shentuo (Beijing) Science & Technology Co. Ltd., Daxing District, Beijing 100176, China*
[5]*School of Mechanical Engineering, Yangtze University, Jingzhou, Hubei 434000, China*

Correspondence should be addressed to Pengcheng Wu; wupengcheng0322@163.com and Chengyu Xia; qlq1010@126.com

Received 24 March 2022; Revised 18 April 2022; Accepted 25 April 2022; Published 20 May 2022

Academic Editor: Punit Gupta

The force and deformation analysis of the bottom hole assembly (BHA) is the foundation and essential component of good trajectory control technology. Still, the BHA structure has complexity (multiangle), making it challenging to analyze the force and deformation of the BHA accurately. In this paper, we consider the factors such as well drilling parameters (drill pressure), drill combination structure parameters (multivariable cross section, stabilizer, and flexible short section diameter and position, etc.), a mechanical analysis model of the push-the-bit rotary steering tool is established based on the infinitesimal method and continuous beam-column theory. Taking the push-the-bit rotary steerable drilling assembly as an example, the influence of force and deformation of the rotary guided drilling assembly, such as drill pressure, stabilizer, and flexible short section parameters, was analyzed. The research results of this paper can solve the mechanical modeling problem of the variable cross section in the bottom drill combination, can deal with the combination of infinite multiple stiffnesses according to the actual situation, bring the analysis results closer to the real problem, and provide theoretical support for the design optimization of the bottom drill combination. In addition, edge computing can provide sufficient computing power for the calculation of this paper to ensure operational efficiency. It can realize the online real-time transmission of mechanical analysis results through powerful calculation examples and effectively guide the field operation.

1. Introduction

The analysis of force and deformation of bottom drilling tool combination is the theoretical basis for the reasonable configuration of the drilling tool combination structure and optimizing drilling operation parameters. It is also of great significance to evaluate the mechanical characteristics of the underground drilling tool, control the hole track, and improve the drilling slope. To realize parameter optimization and improve the oblique-making ability of rotary guide drilling combinations and realize the precise control of the excellent track, it is necessary to establish the mechanical unified theoretical model of rotary guide drilling combination for mechanical analysis and study [1, 2].

In the long-term development process of drilling bottom combinations, many scholars have established many related simplified models and solution methods. According to the equilibrium conditions after the bending deformation, Lubinski et al. [3–5] found the third-order ordinary differential equation for the static analysis of the bottom of the well. They conducted the mechanical analysis of the drilling tools in the well with an inclined plane curve.

Bai et al. [6, 7] simplified the bottom drill tool combination into an interactive elastic continuous beam, studied

the two-dimensional force of the drilling tool combination, and put forward the vertical and horizontal bending methods. Later, Tang et al. [8–10] applied the vertical and horizontal bending method to establish a mechanical model of medium and short radius horizontal shaft-making inclined screw drilling tools and a typical three-dimensional mechanical analysis model of flexible rotary guide drilling tools. Hong et al. [11], combined with the finite element unit division idea and the vertical and horizontal bending beam theory, put forward the generalized vertical and horizontal bending method and completed the mechanical analysis of the combination of noncontinuous rotary guide drilling tools. Hua [12] took the variable stiffness problem of drilling tool combination into account, simplified the combination of single bending screw drilling tool, regarded it as a beam and column subjected to vertical and horizontal bending load, and established the mechanical model of single bending screw drilling tool combination. According to the vertical and horizontal bending beam theory, Shi et al. [13] established the combined mechanical model of the lower drilling rig. Guo et al. [14] optimized the single bending and bistable guide drill combination design according to the quasi-dynamic calculation model of bottom drilling drill combination composite drilling guide force. Zhang et al. [15] built a slope calculation model based on the equilibrium curvature method by considering the influence on the single bending screw drill slope. Hwang et al. [16] used the ANSYS finite element software to establish a mechanical model to simulate the force and deformation of rotary-oriented drilling tools. Liu [17] established a static analysis model for the bottom drill combination of the composite rotary guide drilling tool by using the finite unit method. Zhang and Samuel [18] have established the static analysis model of the bottom drill combination of composite rotary guide drilling tools through the finite unit method. Sehitoglu [19] used simplified mathematical equations to establish the BHA analysis model and optimize the design of BHA.

These scholars have established many mechanical models and methods, but they can only deal with two stiffness problems in one unit. Usually, the number of combined variable sections of the rotary guide drill is more significant than two, which cannot solve the mechanical modeling problem better with more than two variable sections between two stabilizers. Therefore, simplified processing is necessary. Based on these problems, this paper comprehensively considers the drilling parameters (drilling pressure), drilling combination structure parameters (multiple variable sections, stabilizer, and flexible short segment diameter and position, etc.), and other influencing factors and establishes the rotary guide drilling combined mechanical analysis model. The model can carry out the mechanical analysis of the combination of thrust rotary guide drilling tools, which can solve the multisection problem of drilling tools. It is of great significance to analyze the combined mechanical analysis of rotating guide drilling tools according to the real situation to make the analysis results closer to the real situation.

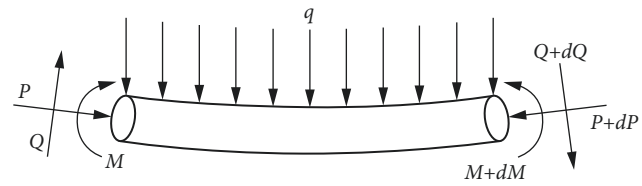

Figure 1: Microforce analysis diagram.

2. Combined Mechanical Model of the Rotary Guide Drill

2.1. Basic Assumption. To establish the combined mechanical model of the rotary guide drill, the following basic assumptions are adopted:

(1) The deformation of the rotary guide drill tool combination composed of drill bit, stabilizer, flexible joint, drill collar, etc. is a small elastic deformation;

(2) The bore diameter is equal to the bit diameter, and the good wall is a rigid body;

(3) The rotary guide drill combination is cut off to the top, and the lower well wall under the influence of dead weight. The torsional deformation of the tip is not considered;

(4) Because of the weight of the combined drill column itself, the part above the cutting point of the drill column falls on the lower well wall;

(5) The contact form between the rotary guide drill tool combination and the excellent wall is the point contact;

(6) The axis of the rotary guide drill is consistent with the bore axis before deformation, and there is an annular gap between that and the good wall;

(7) stabilizer is simplified to the midpoint and the good wall contact the rest of the normal drilling rod;

(8) The wing rib is approximated as a stabilizer with a certain displacement.

2.2. Displacement and Deformation Equation of the Drill Column. To study the influence of variable stiffness on the force deformation of the combination of rotary guide drilling tools, the transverse uniform load and bending moment and axial force are established. The drill bit, variable section, stabilizer, and cutting point of the rotary guide drill tool combination are defined as the node position, and the part between a node and a node is defined as a drill column. The rotary guide drill tool combination can be divided into N section drill columns by $N+1$ nodes. The microelement segment of length d was taken anywhere in the drill tool combination, and the force analysis diagram is shown in Figure 1.

The force balance equation of microelements is (1) [20]:

$$\begin{cases} \sum_{y} = 0 \Rightarrow Q + dQ - Q + q\mathrm{d}x = 0, \\ \sum_{M} = 0 \Rightarrow M - M - dM + Q\mathrm{d}x - \frac{1}{2}q\mathrm{d}x\mathrm{d}x + P\mathrm{d}y = 0. \end{cases} \tag{1}$$

where, P is axial load (N); M is section bending moment (N·m); Q is section shear force, N; q is uniform load ($\mathrm{N\cdot m^{-1}}$); x is the length of the drill column (m); and y is displacement deformation of drill column (m).

The equation for bending moment and curvature is as follows:

$$M = -\mathrm{EI}\frac{\mathrm{d}^2 y}{\mathrm{d}x^2}. \tag{2}$$

Joint (1) and (2) are obtained as follows:

$$\frac{\mathrm{d}^4 y}{\mathrm{d}x^2} + \frac{P}{\mathrm{EI}}\frac{\mathrm{d}^2 y}{\mathrm{d}x^2} = \frac{q}{\mathrm{EI}}. \tag{3}$$

Eq. (3) solves the displacement deformation equation of the microdrill column:

$$y = C_1 + C_2 x + C_3 \cos\left(\sqrt{\frac{P}{\mathrm{EI}}}x\right) + C_4 \sin\left(\sqrt{\frac{P}{\mathrm{EI}}}x\right) + \frac{1}{2}\frac{q}{P}x^2. \tag{4}$$

In (4), E is the elastic modulus of the material (Pa); I is the moment of inertia of the section ($\mathrm{m^4}$); and $C_1'C_2'C_3'C_4$ are unknown constants.

Let $k = \sqrt{P/\mathrm{EI}}$, then (4) is obtained as follows:

$$y = C_1 + C_2 x + C_3 \cos(kx) + C_4 \sin(kx) + \frac{1}{2}\frac{q}{P}x^2. \tag{5}$$

The displacement of the drill column is y, corner cut is $y\prime$, bending moment is $M = EIy\prime\prime$, and shearing force is $F = EIy\prime\prime\prime$.

The displacement deformation equation and the i derivative, the second derivative, and the third derivative:

$$y_i = C_{i1} + C_{i2}x_i + C_{i3}\cos(k_i x_i) + C_{i4}\sin(k_i x_i) + \frac{1}{2}\frac{q_i}{P_i}x_i^2, \tag{6}$$

$$y_i' = C_{i2} - k_i C_{i3}\sin(k_i x_i) + k_i C_{i4}\cos(k_i x_i) + \frac{q_i}{P_i}x_i, \tag{7}$$

$$y_i'' = -k_i^2 C_{i3}\cos(k_i x_i) - k_i^2 C_{i4}\sin(k_i x_i) + \frac{q_i}{P_i}, \tag{8}$$

$$y_i''' = k_i^3 C_{i3}\sin(k_i x_i) - k_i^3 C_{i4}\cos(k_i x_i). \tag{9}$$

The matrix multiplication is in the form of equation set consisting of (6)–(9):

$$\begin{bmatrix} 1 & x_i & \cos(k_i x_i) & \sin(k_i x_i) \\ 0 & 1 & -k_i\sin(k_i x_i) & k_i\cos(k_i x_i) \\ 0 & 0 & -k_i^2\cos(k_i x_i) & -k_i^2\sin(k_i x_i) \\ 0 & 0 & k_i^3\sin(k_i x_i) & -k_i^3\cos(k_i x_i) \end{bmatrix} \bullet \begin{bmatrix} C_{i1} \\ C_{i2} \\ C_{i3} \\ C_{i4} \end{bmatrix} = \begin{bmatrix} y_i - \frac{1}{2}\frac{q_i}{P_i}x_i^2 \\ y_i' - \frac{q_i}{P_i}x_i \\ y_i'' - \frac{q_i}{P_i} \\ y_i''' \end{bmatrix}. \tag{10}$$

The displacement matrix equation of the i section of the rotary guide drill combination and the adjacent latter section (set as section j) can obtain the displacement matrix equation of the two adjacent drill columns as follows:

$$\begin{bmatrix} 1 & x_i & \cos(k_i x_i) & \sin(k_i x_i) & -1 & x_j & \cos(k_j x_j) & sjn(k_j x_j) \\ 0 & 1 & -k_i\sin(k_i x_i) & k_i\cos(k_i x_i) & 0 & -1 & -k_j sjn(k_j x_j) & k_j\cos(k_j x_j) \\ 0 & 0 & -k_i^2\cos(k_i x_i) & -k_i^2\sin(k_i x_i) & 0 & 0 & -k_j^2\cos(k_j x_j) & -k_j^2 sjn(k_j x_j) \\ 0 & 0 & k_i^3\sin(k_i x_i) & -k_i^3\cos(k_i x_i) & 0 & 0 & k_j^3 sjn(k_j x_j) & -k_j^3\cos(k_j x_j) \end{bmatrix} \begin{bmatrix} C_{i1} \\ C_{i2} \\ C_{i3} \\ C_{i4} \\ C_{j1} \\ C_{j2} \\ C_{j3} \\ C_{j4} \end{bmatrix} = \begin{bmatrix} y_i - y_j + \frac{1}{2}\frac{q_i}{P_i}x_i^2 - \frac{1}{2}\frac{q_j}{P_j}x_j^2 \\ y_i' - y_j'' + \frac{q_i}{P_i}x_i - \frac{q_j}{P_j} \\ y_i'' - y_j'' + \frac{q_i}{P_i} - \frac{q_j}{P_j} \\ y_i''' - y_j''' \end{bmatrix}. \tag{11}$$

2.3. Boundary Conditions and Continuity Conditions. The connection mode of rotary guide drill combination can be divided into the following types: articulation connection mode, variable section connection mode, stabilizer connection mode, and tangent connection mode. The boundary conditions and the continuity conditions are described separately for the different connection modes.

(1) Articulated connection mode (only a bit is associated at the bit)

The drill bit is articulated, the displacement y is 0, the bending moment is $EIy'' = 0$. The boundary condition is as follows:

$$\begin{cases} x_i = 0, & y_i = 0, \\ x_i = 0, & y_i'' = 0. \end{cases} \tag{12}$$

(13) is obtained by substituting (12) into (11):

$$\begin{bmatrix} 1 & 0 & 1 & 0 \\ 0 & 0 & k_i^2 & 0 \end{bmatrix} \begin{bmatrix} C_{i1} \\ C_{i2} \\ C_{i3} \\ C_{i4} \end{bmatrix} = \begin{bmatrix} 0 \\ -\dfrac{q_i}{P_i} \end{bmatrix}. \tag{13}$$

(2) Variable the cross section connection mode (At the variable section between the drill columns, associate two drill columns)

Any adjacent two drill columns have equal displacement, rotation angle, bending moment, and shear force at their variable section node, the boundary conditions and the continuity conditions are as follows:

$$\begin{cases} x_i = L_i, & x_j = 0,\ y_i = y_j, \\ x_i = L_i, & x_j = 0,\ y_i' = y_j', \\ x_i = L_i, & x_j = 0,\ E_i I_i I y_i'' = E_j I_j y_j'', \\ x_i = L_i, & x_j = 0,\ E_i I_i I y_i''' = E_j I_j y_j'''. \end{cases} \tag{14}$$

(15) is obtained by substituting (14) into (11):

$$\begin{bmatrix} 1 & L_i & \cos(k_i L_i) & \sin(k_i L_i) & -1 & 0 & -1 & 0 \\ 0 & 1 & -k_i \sin(k_i L_i) & k_i \cos(k_i L_i) & 0 & -1 & 0 & -k_j \\ 0 & 0 & -E_i I_i k_i^2 \cos(k_i L_i) & -E_i I_i k_i^2 \sin(k_i L_i) & 0 & 0 & E_j I_j k_j^2 & 0 \\ 0 & 0 & E_i I_i k_i^3 \sin(k_i L_i) & -E_i I_i k_i^3 \cos(k_i L_i) & 0 & 0 & 0 & E_j I_j k_j^2 \end{bmatrix} \begin{bmatrix} C_{i1} \\ C_{i2} \\ C_{i3} \\ C_{i4} \\ C_{j1} \\ C_{j2} \\ C_{j3} \\ C_{j4} \end{bmatrix} = \begin{bmatrix} -\dfrac{1}{2}\dfrac{q_i}{P_i} L_i^2 \\ -\dfrac{q_i}{P_i} L_i \\ -E_i I_i \dfrac{q_i}{P_i} + E_j I_j \dfrac{q_j}{P_j} \\ 0 \end{bmatrix}. \tag{15}$$

(3) Stabilizer connection mode (The stabilizer contacts with the well wall and connects the two drill columns)

The two drill columns on the left and right sides of the stabilizer shift, angle, bending moment, and shear at the stabilizer node are both equal, and the displacement is equal to half of the difference between the wellbore diameter and the outer diameter of the stabilizer. The boundary conditions and their continuity conditions are as follows:

$$\begin{cases} x_i = L_i, & x_j = 0,\ y_i = y_j, \\ x_i = L_i, & y_i = \dfrac{d_1 - d_i}{2}, \\ x_i = L_i, & x_j = 0,\ y_i' = y_j' \\ x_i = L_i, & x_j = 0,\ E_i I_i I y_i'' = E_j I_j y_j'' \end{cases} \tag{16}$$

(17) is obtained by substituting (16) into (11):

$$\begin{bmatrix} 1 & L_i & \cos(k_iL_i) & \sin(k_iL_i) & -1 & 0 & -1 & 0 \\ 1 & L_i & \cos(k_iL_i) & \sin(k_iL_i) & 0 & 0 & 0 & 0 \\ 0 & 0 & -k_i\sin(k_iL_i) & k_i\cos(k_iL_i) & 0 & -1 & 0 & -k_j \\ 0 & 0 & -E_iI_ik_i^2\cos(k_iL_i) & -E_iI_ik_i^2\sin(k_iL_i) & 0 & 0 & E_jI_jk_j^2 & 0 \end{bmatrix} \begin{bmatrix} C_{i1} \\ C_{i2} \\ C_{i3} \\ C_{i4} \\ C_{j1} \\ C_{j2} \\ C_{j3} \\ C_{j4} \end{bmatrix} = \begin{bmatrix} -\frac{1}{2}\frac{q_i}{P_i}L_i^2 \\ \frac{d_1-d_i}{2} - \frac{1}{2}\frac{q_i}{P_i}x_i^2 \\ -\frac{q_i}{P_i}L_i \\ -E_iI_i\frac{q_i}{P_i} + E_jI_j\frac{q_j}{P_j} \end{bmatrix}. \tag{17}$$

(5) Tangent connection mode (cut point and well wall cut, associated with a section of drilling column)

At the cut point, the corner is 0, the displacement is equal to half the difference between the bore diameter and the bore diameter, the boundary conditions and continuity conditions are as follows:

$$\begin{cases} x_i = L_i, \quad y_i = \dfrac{d_1 - d_i}{2}, \\ x_i = L_i, \quad y_i' = 0. \end{cases} \tag{18}$$

(19) is obtained by substituting (18) into (11):

$$\begin{bmatrix} 1 & L_i & \cos(k_iL_i) & \sin(k_iL_i) \\ 0 & 1 & -k_i\sin(k_iL_i) & k_i\cos(k_iL_i) \end{bmatrix} \bullet \begin{bmatrix} C_{i1} \\ C_{i2} \\ C_{i3} \\ C_{i4} \end{bmatrix} = \begin{bmatrix} \frac{d_1-d_i}{2} - \frac{1}{2}\frac{q_i}{P_i}x_i^2 \\ -\frac{q_i}{P_i} \end{bmatrix}. \tag{19}$$

2.4. Flowchart. For the combination of rotary guide drills divided into N segments, according to the boundary conditions and continuity condition equations at $N+1$ nodes, a system of equations containing 4N equations containing 4N unknowns can be obtained. A mechanical model to form a linear matrix equation AX = B:

$$\begin{bmatrix} A_0 & O & O & & & & \\ A_{11} & A_{12} & O & \cdots & & O & \\ O & A_{21} & A_{22} & & & & \\ \vdots & & \ddots & & \vdots & & \\ & & & A_{(N-2)1} & A_{(N-2)2} & O & \\ & O & \cdots & O & A_{(N-1)1} & A_{(N-1)1} & \\ & & & O & O & A_N & \end{bmatrix} \bullet \begin{bmatrix} X_1 \\ X_2 \\ X_3 \\ \vdots \\ X_{N-2} \\ X_{N-1} \\ X_N \end{bmatrix} = \begin{bmatrix} B_0 \\ B_1 \\ B_2 \\ \vdots \\ B_{N-2} \\ B_{N-1} \\ B_N \end{bmatrix}, \tag{20}$$

where A_0 is 2×4 matrix, it is the boundary condition coefficient matrix at the first node (drill bit node); $A_i = (A_{i1}|A_{i2})$ is 4×8 matrix ($i = 1, 2, \ldots, N-1$), it is the matrix of boundary condition coefficients at the $i+1$ node; A_N is 2×4 matrix, it is the boundary condition coefficient matrix at the $N+1$ node (cut point node). $X_i = [C_{i1}, C_{i2}, C_{i3}, C_{i4}]'$ is 4×1 matrix, it is the unknown number coefficient matrix of the displacement function in segment i. B_0 is 2×1 matrix, it is the boundary condition constant matrix at the first node (drill bit node); B_i is 4×1 matrix ($i = 1, 2, \ldots, N-1$) it is the boundary condition constant matrix at the $i+1$ node; B_N is 2×1 matrix, it is the boundary condition constant matrix at the $N+1$ node (cut point node).

Any combination of rotary guide drills is divided into multiple drill columns according to the node position, and then the node connection mode is determined. Then, using the idea of finite element, the matrix equations of boundary conditions of each node can be established together. It includes a linear matrix equation AX = B and a nonlinear equation EIK = M at a tangent point. Finally, the combined overall equation can be obtained through the iterative search solution. The flowchart is shown in Figure 2.

3. Analysis of Combined Mechanical Properties of the Sliding Rotary Guide Drill

To analyze the influence of the drilling pressure drilling, stabilizer, and flexible short segment parameters of different guide wing rib extension elongation on the lateral force at the drill bit during the rotary guide drill combination composite drilling. This paper uses the combination of static push-back rotary guide drills as shown in Figure 3. Its structure parameters are as follows: Φ215.9 mm PDC bit + Φ197 mm rotation guide tool + Φ187 mm drill collar + Φ212 mm stabilator+ Φ135 mm flexible short section + Φ171.45 mm non-magnetic drill collar. The specific parameters are shown in Table 1.

3.1. Effect of the Guide Wing Rib Extension Length on the Lateral Force of the Drill Bit. Only the length of the guide

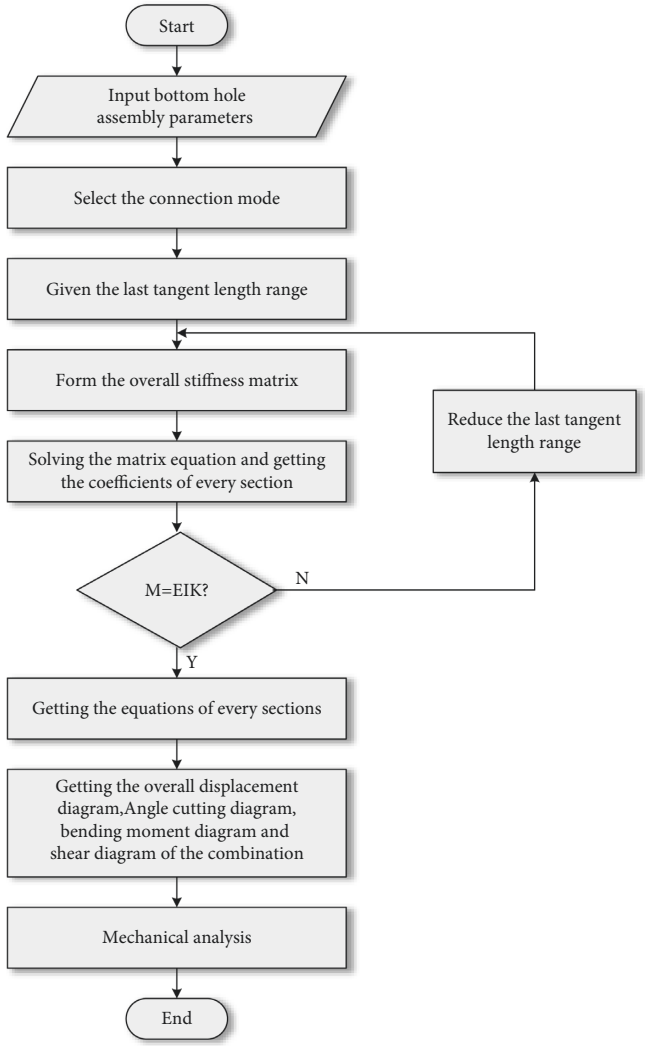

Figure 2: Flowchart.

wing rib was changed to analyze the influence of the lateral force under different flexible short segments. The results are shown in Figure 4. According to the figure, the lateral force increases with the extended length of the guide wing ribs. Therefore, the extension length of the guide wing rib should be appropriately increased to increase the lateral force.

3.2. Effect of the Flexible Short Segment Length on the Lateral Force of the Drill Bit. Only the length of the flexible segment was changed, and the influence of the lateral force at the bit was analyzed. The results are shown in Figure 5. As can be seen from the figure, the lateral force increases with the length of the short flexible segment at different distances of the stabilizer above the short flexible segment. It increases with the stabilizer distance above the short flexible segment. Therefore, the length of the flexible segment should be appropriately increased, and the distance between the flexible segment stabilizer should be increased to increase the lateral force.

3.3. Effect of Drilling Pressure on the Lateral Force of the Drill Bit. Only the size of the drilling pressure was changed to analyze the influence of different drilling pressure on the lateral force at the drill bit. The results are shown in Figure 6. As shown from the figure, under different guide wing rib extension lengths, the lateral force is not significantly changed when the drilling pressure increases. The drilling pressure has little influence on the lateral force.

3.4. Effect of Upper Stabilizer Diameter on Lateral Force of Drill Bit. The influence of the different stabilizer diameters on the lateral force of the bit is analyzed, and the results are shown in Figure 7. According to the figure, the lateral force increases with the diameter of the upper stabilizer at different

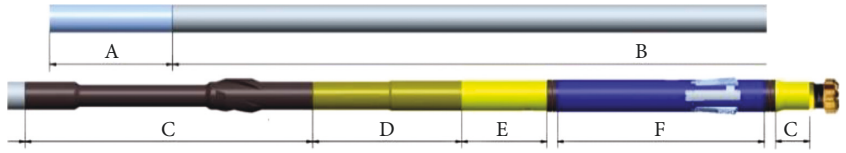

Figure 3: Schematic diagram of static thrust type rotary guide drill combination.

Table 1: Specific parameters of rotary guide drill combination.

Parameter	Value (unit)
(A) PDC drill bit diameter/length	215.9 (mm)/0.25 (m)
(G) lower joint diameter/length	171 (mm)/0.2065 (m)
(F) diameter/length of the rotary guide tool	197 (mm)/1.63 (m)
(E) central pipe diameter/length	187 (mm)/1.24 (m)
(D) drilling collar diameter/length	171.45 (mm)/1.42 (m)
Stabilizer diameter	212 (mm)
(C) flexible short section diameter/length	135 (mm)/1.03 (m)
(B) No drill-free collar diameter/length	171.45 (mm)/7.776 (m)
Bit weight	120 (kN)
Density of drilling fluid	1.13 ($kg{\cdot}L^{-1}$)

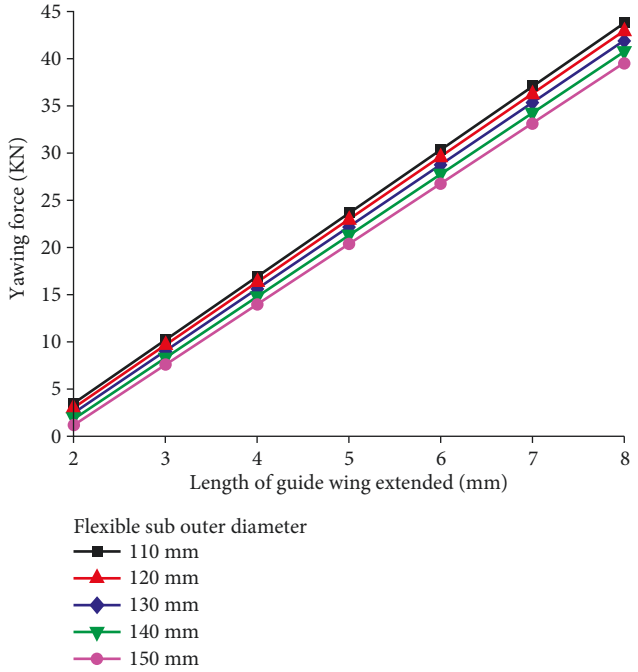

Figure 4: Effect of the protruding length of the guide wing rib on the lateral force at the drill bit.

protruding lengths of the guide wing ribs. Therefore, the upper stabilizer diameter should be appropriately increased to increase the lateral force.

3.5. Effect of the Drill Bit to the Guide Wing Rib Distance on the Lateral Force of the Drill Bit. The influence of the distance between bit and guide wing ribs on the lateral force at the drill bit and the results are shown in Figure 8. According to

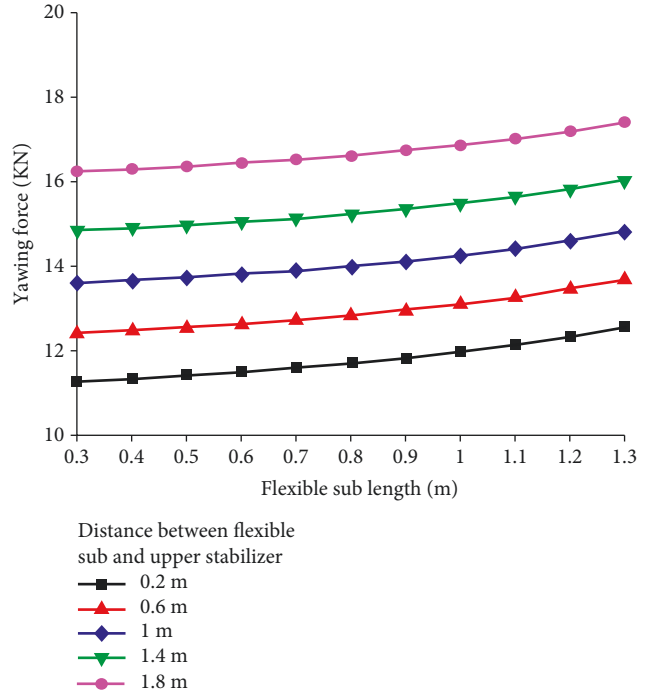

Figure 5: Effect of the flexible short segment length on the lateral force at the drill bit.

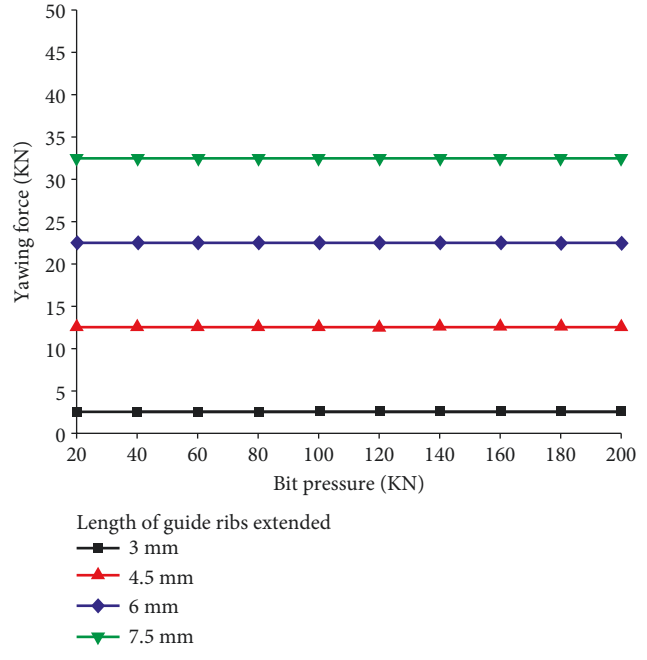

Figure 6: Effect of drill pressure on the lateral force at the drill bit.

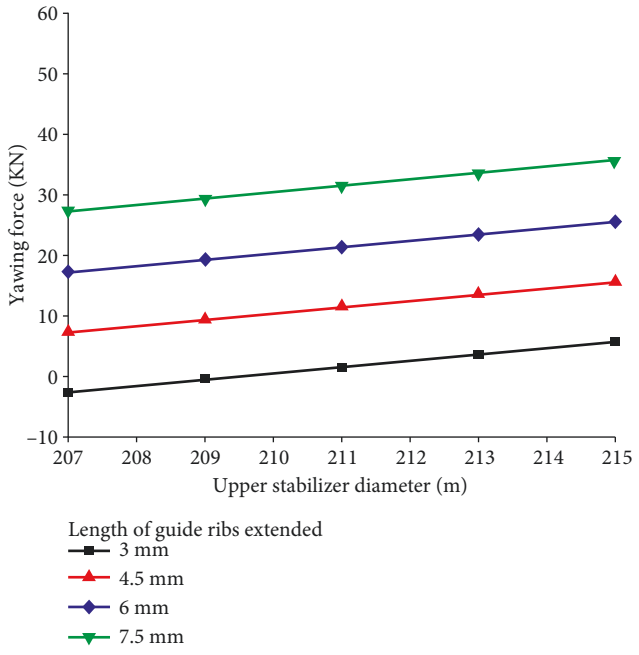

Figure 7: Effect of the upper stabilizer diameter on the lateral force at the drill bit.

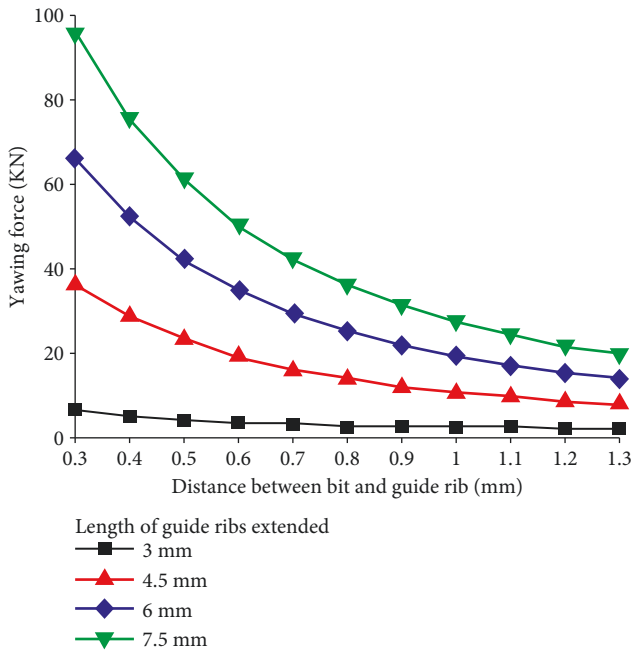

Figure 8: Effect of distance from drill to guide ribs on the lateral force at the bit.

the figure, the lateral force decreases with the distance between the drill to the guide rib at different lengths of the guide ribs. Therefore, the distance between the drill bit and the guide wing rib should be appropriately reduced to increase the lateral force.

4. Conclusion

Based on the microelement method and continuous beam theory, the influencing factors of borehole drilling parameters (drilling pressure), combined structure parameters (diameter and position, stabilizer, and flexible short section) are used to establish the combined mechanical analysis model of a rotary-guide drill tool. According to the rotary guide drill's established combined mechanical analysis model, the sliding rotary guide combination influences drilling pressure, stabilizer, and flexible short section parameters on the force and deformation of the rotary guide drill combination are analyzed. The conclusion is as follows:

(1) Among the factors affecting the combined slope ability of the guide drill, the drill distance to the stabilizer has more influence on the composite drilling slope, the stabilizer diameter is the second, the adjustable short section length and outer diameter have less influence on the slope, and the drilling pressure on the slope is very small.

(2) With the protruding length of the guide wing rib, the diameter of the upper stabilizer, and the flexible short joint distance of the upper stabilizer increases, the lateral force at the drill bit increases. With the protruding length of the guide wing rib, the diameter of the upper stabilizer, and the distance of the upper stabilizer increases, the lateral force at the drill bit increases. With the outer diameter of the flexible short section and the distance between the drill to the guide wing rib, the lateral force at the bit decreases. As the drill pressure increases, the lateral force at the drill bit changes a little.

Using the established combined mechanical analysis model of the rotary guide drilling tool, the mechanical analysis of the thrust type rotary guide drilling tool combination can be conducted to solve the multisection problem of the drilling tool combination. Then, it can deal with infinitely many stiffness drilling combinations according to the real situation so that the analysis results are closer to the real situation. The research results are of great significance to the mechanical characteristics of underground drilling tools, control of well hole track, improving drilling speed and construction slope, and can also provide theoretical support for the design and optimization of the combination of thrust rotary guide drilling tools.

Data Availability

The datasets used and/or analyzed during the current study are available from the corresponding author on reasonable request.

Conflicts of Interest

The authors declare that they have no conflicts of interest.

References

[1] C. Zou, G. Zhai, G. Zhang et al., "Formation, distribution, potential and prediction of global conventional and unconventional hydrocarbon resources," *Petroleum Exploration and Development*, vol. 42, no. 01, pp. 14–28, 2015.

[2] J. Marck and E. Detournay, "Influence of rotary-steerable-system design on borehole s," *SPE Journal*, vol. 21, no. 01, pp. 293–302, 2016.

[3] A. Lubinski, "A Study of Buckling of Rotary Drilling," *Drilling and production*, pp. 178–214, 1951.

[4] H. Niemi, "Teacher Effectiveness in the European Context with a Special Reference to Finland," 2015.

[5] H. Wang, Z. C. Guan, Y. C. Shi, and Y. Liu, "Drilling trajectory prediction model for push-the-bit rotary steerable bottom hole assembly," *International Journal of Engineering, Transactions B: Applications*, vol. 30, no. 11, pp. 1800–1806, 2017.

[6] J. Bai, "Bottom hole assembly problems solved by beam-column theory," in *Proceedings of the International Petroleum Exhibition and Technical Symposium*, pp. 106–116, Beijing, China, March 1982.

[7] J. Bai and Y. Su, *Deviation Control in Direction Drilling*, pp. 61-62, China Petroleum Industry Press, Beijing, China, 1990.

[8] X. Tang, "Non-uniform stiffness beam-columntheory and its application," *Mechanics in Engineering*, vol. 33, no. 05, pp. 12–15, 2011.

[9] X. Tang, Y. Su, and Z. Chen, "Beam-column theory for bent housing PDM assemblies with medium-short radius of building capability," *Mechanics in Engineering*, vol. 33, no. 3, pp. 20–24, 2011.

[10] X. Tang, Y. Su, Y. Ge, L. Sheng, and T. Li, "BHA Mechanical analysis for rotary steering drilling system," *Mechanics in Engineering*, vol. 35, no. 01, pp. 55–59, 2013.

[11] D. Hong, X. Tang, Y. Su, L. Shen, and X. Dou, "Generalized beam-column method for non-continuous rotary steering drilling of bottom-hole assembly," *Acta Petrolei Sinica*, vol. 35, no. 03, pp. 543–550, 2014.

[12] Y. Hua, *Force Analysis and Build-Up Rate Prediction of Single Bend PDM Drill Assembly*, Yangtze University, Jingzhou, China, 2018.

[13] Y. Shi, Z. Teng, B. Jing et al., "Improved mechanical model of the static push-the-bit rotary steerable bottom-hole assembly," *Journal of China University of Petroleum (Edition of Natural Science)*, vol. 42, no. 5, pp. 75–80, 2018.

[14] Z. Guo, D. Gao, and H. Zhang, "Analysis and optimization of holding-inclination capability of steerable assembly with single bend and two stabilizers," *Petroleum Drilling Techniques*, vol. 41, no. 06, pp. 19–24, 2013.

[15] R. Zhang, J. He, J. Liu, and D. Ma, "Study on build-up capacity of positive displacement drill (PDD) with single bend zhang hui," *Journal of Yangtze University (Natural Science Edition)*, vol. 13, no. 02, pp. 41–46, 2016.

[16] Y. M. Hwang, K. S. Jhuang, and H. C. Yu, "Finite element simulation of rotating compression forming," *Materials Science Forum*, vol. 920, pp. 22–27, 2018.

[17] J. Liu, *Analysis and Design of Build-Up Capacity of Compound Rotary Steerable Drilling Tools*, Xi'an Shiyou University, Xian, China, 2018.

[18] Y. Zhang and R. Samuel, "Analytical Model to Estimate the Directional Tendency of point and Push-The-Bit BHAs," in *Proceedings of the SPE Annual Technical Conference and Exhibition. Society of Petroleum Engineers*, TX, USA, September 2015.

[19] H. Sehitoglu, "Optimal control system design with prescribed damping and stability characteristics," *Journal of Guidance, Control, and Dynamics*, vol. 16, no. 6, pp. 1183–1185, 1993.

[20] I. Nobuyuki and K. Takashi, "Large deformation analysis and synthesis of elastic closed-loop mechanism made of a certain spring wire described by free curves," *Chinese Journal of Mechanical Engineering*, vol. 28, no. 4, pp. 756–762, 2015.